

Metallosite Selectivity Studies in Reactions of Tetrahedral MCo_3 Carbonyl Clusters ($\text{M} = \text{Fe}, \text{Ru}$) with Cyclohexylphosphine. Skeletal Rearrangements Leading to Tri- and Pentanuclear Phosphinidene Clusters and Crystal Structures of $\text{RuCo}_4(\mu_4\text{-PCy})(\mu\text{-CO})_2(\text{CO})_{11}$ and $\text{RuCo}_2(\mu_3\text{-PCy})(\text{CO})_9^\dagger$

Soraya Bouherour, Pierre Braunstein,* and Jacky Rosé*

Laboratoire de Chimie de Coordination, UMR 7513 CNRS, Université Louis Pasteur, 4 rue Blaise Pascal, 67070 Strasbourg Cédex, France

Loïc Toupet

Groupe Matières Condensée et Matériaux, UMR 6626 CNRS, Université de Rennes I, Avenue du Général Leclerc, 35042 Rennes Cédex, France

Received April 21, 1999

We have studied the metallosite selectivity of substitution reactions at heterometallic tetranuclear clusters of the type $\text{HMCo}_3(\text{CO})_{12}$ ($\text{M} = \text{Fe}, \text{Ru}$). Monosubstitution with PCyH_2 occurs with a different metallosite selectivity as a function of M . When $\text{M} = \text{Fe}$, substitution of a Co-bound CO ligand occurs whereas when $\text{M} = \text{Ru}$, the phosphine ligand is bound to Ru. Introduction of a second substituent (PCyH_2 or NMe_3) occurs in both cases at cobalt and, in the case of $\text{HFeCo}_3(\text{CO})_{11}(\text{PCyH}_2)$, at a cobalt that does not carry the PCyH_2 substituent. The clusters $\text{HMCo}_3(\text{CO})_{11}(\text{PCyH}_2)$ (**2a**, $\text{M} = \text{Fe}$; **2b**, $\text{M} = \text{Ru}$) transform in solution to give the corresponding μ_3 -phosphinidene-capped heterotrinnuclear clusters $\text{MCo}_2(\mu_3\text{-PCy})(\text{CO})_9$ (**4a**, $\text{M} = \text{Fe}$; **4b**, $\text{M} = \text{Ru}$). The μ_4 -phosphinidene-capped intermediate $\text{RuCo}_4(\mu_4\text{-PCy})(\mu\text{-CO})_2(\text{CO})_{11}$ (**5b**) could be fully characterized, whereas the analogous species could not be isolated when $\text{M} = \text{Fe}$. The transformation of **2a,b** was accelerated by addition of Me_3NO . This work demonstrates that a reaction which represents a partial cluster fragmentation, with a nuclearity change from 4 to 3, may occur via the intermediacy of a larger cluster, of nuclearity 5. Reactions and products were studied by IR and ^1H , $^{31}\text{P}\{^1\text{H}\}$, and ^{59}Co NMR spectroscopic methods, and the clusters **4b** and **5b** have been characterized by X-ray diffraction.

Introduction

Phosphines are among the most ubiquitous ligands in transition-metal chemistry and are known to significantly alter the structure and/or reactivity of their metal complexes, in both stoichiometric and catalytic reactions. This has been examined in considerable detail in mononuclear chemistry and to a large extent with homonuclear metal clusters. Mixed-metal clusters have been increasingly used in catalysis, and there is evidence that cooperative effects may lead to improved properties compared to homometallic systems.¹ Furthermore, heterometallic clusters provide unique op-

portunities for studying the synthesis and reactivity of isomers which differ by the nature of the metal to which a given ligand is bound. As a result, investigations concerning the metallosite selectivity of mixed-metal clusters have become of increasing importance and we have recently reported on such aspects.² The tetrahedral carbonyl clusters $\text{HMCo}_3(\text{CO})_{12}$ ($\text{M} = \text{Fe}$, **1a**; $\text{M} = \text{Ru}$, **1b**) have proven particularly suitable for such studies, as they are amenable to $^{31}\text{P}\{^1\text{H}\}$ and ^{59}Co NMR investigations.³ In addition, these clusters have received much attention as catalyst precursors in CO/H_2 and methanol homologation chemistry.¹ They have been studied in heterogeneous and homogeneous media, and in the latter case, phosphine ligands have been shown to enhance their activity/selectivity. However, the exact nature of the phosphine-substituted clusters present

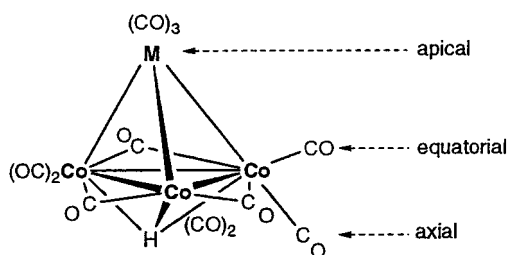
[†] Dedicated to our friend and colleague Professor Daniel Grandjean (University Rennes I), on the occasion of his retirement, with our best wishes.

* To whom correspondence should be addressed. E-mail: braunst@chimie.u-strasbg.fr.

(1) (a) Braunstein, P.; Rosé, J. In *Catalysis by Di- and Polynuclear Metal Cluster Complexes: Heterometallic Clusters for Heterogeneous Catalysis*; Adams, R. D., Cotton, F. A., Eds.; Wiley-VCH: New York, 1998; p 443. (b) Braunstein, P.; Rosé, J. In *Comprehensive Organometallic Chemistry II*; Abel, E. W., Stone, F. G. A., Wilkinson, G., Eds.; Pergamon Press: Oxford, 1995; Vol. 10, pp 351–385. (c) Braunstein, P.; Rosé, J. In *Metal Clusters in Chemistry*; Braunstein, P., Raithby, P. R., Oro, L. A., Eds.; Wiley-VCH: Weinheim, Germany, 1999; Vol. 2, pp 616–677.

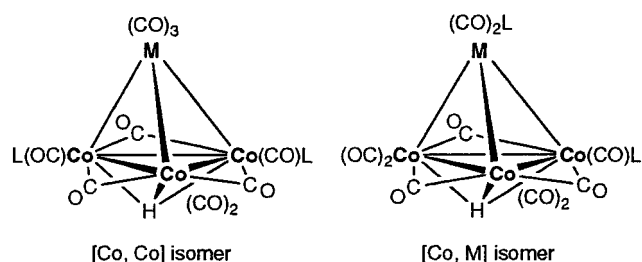
(2) (a) Braunstein, P.; Rosé, J.; Granger, P.; Raya, J.; Bouaoud, S.-E.; Grandjean, D. *Organometallics* **1991**, *10*, 3686. (b) Braunstein, P.; Mourey, L.; Rosé, J.; Granger, P.; Richert, T.; Balegroune, F.; Grandjean, D. *Organometallics* **1992**, *11*, 2628. (c) Braunstein, P.; Rosé, J.; Toussaint, D.; Jääskeläinen, S.; Ahlgren, M.; Pakkanen, T. A.; Pursiainen, J.; Toupet, L.; Grandjean, D. *Organometallics* **1994**, *13*, 2472. (3) (a) Granger, P.; Elbayed, K.; Raya, J.; Kempgens, P.; Rosé, J. *J. Magn. Reson.* **1995**, *117*, 179. (b) Richert, T.; Elbayed, K.; Raya, J.; Granger, P.; Braunstein, P.; Rosé, J. *Magn. Reson. Chem.* **1996**, *34*, 689.

Scheme 1



under catalytic conditions has rarely been determined. For these tetrahedral clusters, stepwise addition of monophosphine ligands may lead to the incorporation of up to three ligands. Carbonyl substitution readily takes place, and the interplay between the changes in kinetic and thermodynamic parameters resulting from phosphine substitution generally leads to complete chemo- and stereoselectivity. Thus, previous studies with **1a** and **1b** have shown that CO monosubstitution by tertiary or secondary phosphine ligands takes place exclusively at one of the three equivalent Co atoms. The combined use of spectroscopic methods in solution, such as ^1H , $^{31}\text{P}\{^1\text{H}\}$, and ^{59}Co NMR, with solid-state studies by $^{31}\text{P}\{^1\text{H}\}$ and ^{59}Co NMR and X-ray diffraction allows a better monitoring of the reactions and an understanding of the selectivity for apical vs basal substitution, which in the latter case may occur in an axial or equatorial position (Scheme 1).

In such monosubstituted clusters, all observations so far indicate that the phosphorus ligand is bound to cobalt in an axial position. Disubstitution only leads to the axial $[\text{Co}, \text{Co}]$ isomer of $\text{HMCo}_3(\text{CO})_{10}\text{L}_2$ (L = phosphine), whereas both $[\text{Co}, \text{Co}]$ and $[\text{Co}, \text{Ru}]$ isomers may be observed in the case of **1b**, depending on the nature of the phosphine used:



Trisubstitution of **1a** with $\text{P}(\text{OMe})_3$ has been established by X-ray and neutron diffraction to occur at the cobalt centers (one phosphite on each cobalt center).⁴ In the reaction products of **1b** with various phosphines, one of the three ligands is always bonded to ruthenium.^{2c,5} The affinity toward phosphines decreases in the order $\text{Co} > \text{Ru} > \text{Fe}$.

The majority of such studies have been concerned with tertiary phosphines, and whereas there have been a few examples dealing with the reactivity of secondary phosphines, relatively little is known about the behavior of primary phosphines PRH_2 . The latter ligands could lead to simple CO substitution or formation of organo-phosphido- (μ -PRH) or phosphinidene-based (μ_3 -PR)

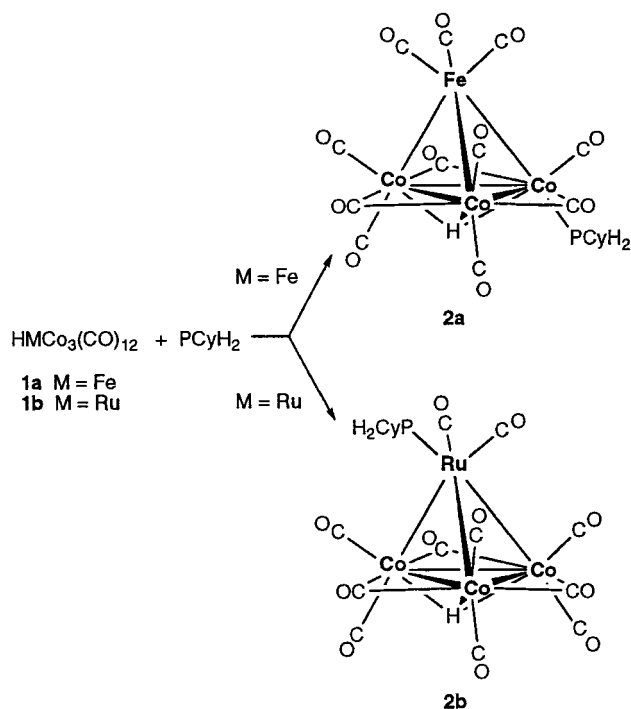
polynuclear compounds via P–H oxidative addition. Although such reactions have been observed with homo- and heterotrimeric clusters,⁶ there seems to have been no report on related chemistry involving tetrahedral mixed-metal carbonyl clusters. Here we present a study on the reactivity of **1a** and **1b** toward PCyH_2 which led to unprecedented metallosite selectivity and the characterization of metal core rearrangements leading to new tri- and pentanuclear clusters.

Results and Discussion

The reaction of $\text{HMCo}_3(\text{CO})_{12}$ (**1a**, $\text{M} = \text{Fe}$; **1b**, $\text{M} = \text{Ru}$) with 1 equiv of PCyH_2 in dichloromethane at room temperature led to the formation of $\text{HMCo}_3(\text{CO})_{11}(\text{PCyH}_2)$ (**2a**, $\text{M} = \text{Fe}$; **2b**, $\text{M} = \text{Ru}$), which were characterized by analytical and spectroscopic data (Table 1).

As reported earlier, the reactions of **1a** and **1b** with various tertiary or secondary phosphines lead to monosubstituted derivatives, in which the phosphine ligand is always axially bound to a cobalt center.² Variation in the nature of the phosphine ligand results only in slight changes in the IR patterns of the products. Although the IR spectra in the $\nu(\text{CO})$ region of cobalt-substituted FeCo_3 and RuCo_3 clusters of the type $\text{HMCo}_3(\text{CO})_{11}\text{L}$ are always very similar, the IR spectra of **2a** and **2b** showed notable differences which point to the presence of two isomers (Scheme 2). The Fe-

Scheme 2



containing cluster **2a** was spectroscopically characterized as the axially Co-bound isomer, by analogy with the data for $\text{HFeCo}_3(\text{CO})_{11}(\text{PPh}_2\text{H})$, the structure of which has been established by X-ray diffraction.^{2a} The

(4) (a) Huie, B. T.; Knobler, C. B.; Kaesz, H. D. *J. Am. Chem. Soc.* **1978**, *100*, 3059. (b) Teller, R. G.; Wilson, R. D.; McMullan, R. K.; Koetzle, T. F.; Bau, R. *J. Am. Chem. Soc.* **1978**, *100*, 3071.

(5) Bouherour, S.; Braunstein, P.; Rosé, J., unpublished results.

(6) (a) Natarajan, K.; Zsolnai, L.; Huttner, G. *J. Organomet. Chem.* **1981**, *220*, 365. (b) Iwasaki, F.; Mays, M. J.; Raithby, P. R.; Taylor, P. L.; Wheatley, P. J. *J. Organomet. Chem.* **1981**, *213*, 185. (c) Field, J. S.; Haines, R. J.; Smit, D. N. *J. Organomet. Chem.* **1982**, *224*, C49. (d) Field, J. S.; Haines, R. J.; Smit, D. N. *J. Organomet. Chem.* **1986**, *304*, C17. (e) Roland, E.; Bernhardt, W.; Vahrenkamp, H. *Chem. Ber.* **1986**, *119*, 2566.

Table 1. Selected IR and NMR Data

cluster	IR $\nu(\text{CO})$, cm^{-1}	^1H NMR δ , ppm ^d	$^{31}\text{P}\{^1\text{H}\}$ NMR δ , ppm ($\Delta_{1/2}$, Hz) ^d	^{59}Co NMR δ , ppm ($\Delta_{1/2}$, Hz) ^d
HFeCo ₃ (CO) ₁₂ (1a)	2060 vs, 2052 vs, 2030 m, 1990 m, 1887 s ^c	−21.5 (s, $\mu_3\text{-H}$)		−2720 (420, Co–CO) ^e
HFeCo ₃ (CO) ₁₁ (PCyH ₂) (Co) (2a)	2080 m, 2036 vs, 2016 s, 1977 m, 1902 w, 1874 m, 1860 m ^c	−21.4 (s, $\mu_3\text{-H}$), 1.24 and 1.80 (2 m, 11H, Cy), 3.2 (dd, PH ₂ , 2H, $^1J_{\text{P-H}} = 330$ Hz, $^3J_{\text{H-H}} = 5$ Hz)	−40 (s, P–Co, 3200)	−2719 (1800, 2 Co–CO), −2674 (1800, 1 Co–P)
HFeCo ₃ (CO) ₁₀ (PCyH ₂) ₂ (Co, Co) (3a)	2061 s, 2022 vs, 2003 vs, 1966 m, 1863 w, 1854 m, 1839 m ^a	−21.9 (s, $\mu_3\text{-H}$), 1.32 and 1.82 (2 m, 11H, Cy), 3.72 (dd, PH ₂ , 2H, $^1J_{\text{P-H}} = 312$ Hz, $^4J_{\text{P-H}} = 56$ Hz)	−38 (m, P–Co, 2800)	−2727 (1970, Co–CO), −2629 (1350, Co–P)
FeCo ₂ ($\mu_3\text{-PCy}$)(CO) ₉ (5a)	2092 m, 2047 vs, 2037 vs, 2030 vs, 2010 w, 2006 sh, 1981 m, 1967 m ^a		483 (s, $\mu_3\text{-P}$, 410)	−2957 (10 000)
HRuCo ₃ (CO) ₁₂ (1b)	2067 vs, 2024 m, 1879 m ^c	−19.7 (s, $\mu_3\text{-H}$)		−2760 (1700, Co–CO)
HRuCo ₃ (CO) ₁₁ (PCyH ₂) (Ru) (2b)	2078 m, 2043 s, 2028 s, 1985 m, 1880 m, 1868 m ^c	−18.2 ($\mu_3\text{-H}$), 0.9, 1.27, and 1.90 (3 m, 11H, Cy), 4.33 (dd, PH ₂ , 2H, $^1J_{\text{P-H}} = 354$ Hz, $^3J_{\text{H-H}} = 5$ Hz)	−19.7 (s, P–Ru, 50)	−2790 (8300, Co–CO)
HRuCo ₃ (CO) ₁₀ (PCyH ₂) ₂ (Co, Ru) (3b)	2054 s, 2014 vs, 1970 m, 1850 m, 1835 sh ^c	−18.6 (s, $\mu_3\text{-H}$), 0.8–0.9, 1.52–1.8, (3 m, 22H, Cy), 4.0 (d, PH ₂ , 2H, $^1J_{\text{P-H}} = 329$ Hz, $^3J_{\text{H-H}} = 5$ Hz), 4.3 (d, PH ₂ , 2H, $^1J_{\text{P-H}} = 350$ Hz, $^3J_{\text{H-H}} = 11$ Hz)	−23.4 (d, P–Ru, $^3J_{\text{P-P}} = 50$ Hz), P–Co too broad to be assigned	−2774 (5750, Co–CO + Co–P)
RuCo ₄ ($\mu_4\text{-PCy}$)(CO) ₁₃ (4b)	2088 w, 2054 vs, 2036 sh, 2033 vs, 2020 w, 2012 w, 1987 w, 1867 m ^a		too unstable	−1805 (7000, Co–CO + Co–P)
RuCo ₂ ($\mu_3\text{-PCy}$)(CO) ₉ (5b)	2091 s, 2049 vs, 2043 vs, 2028 vs, 2026 m, 2009 m, 1980 m ^a	1.6, 1.96, and 2.35 (3m, 11H, Cy)	450 (s, $\mu_3\text{-P}$, 530)	−3030 (10 000)
HRuCo ₃ (CO) ₁₀ (PCyH ₂)-(NMe ₃) (Co, Ru) (6b)	2049 m, 1999 vs, 1985 sh, 1964 s, 1941 s, 1868 m, 1846 s, 1824 s ^b	too unstable	too unstable	−2780 (6800, Co–CO), −1360 (3400, Co–N), −1150 (4000, Co–N)

^a In hexane. ^b In KBr. ^c In CH₂Cl₂. ^d In CDCl₃. ^e In CD₂Cl₂.

situation appears different for the Ru-containing cluster **2b** and, on the basis of ^1H , $^{31}\text{P}\{^1\text{H}\}$, and ^{59}Co NMR data (see Table 1) and by comparison with the structurally characterized cluster HRuCo₃(CO)₁₁(TeMe₂),⁷ we suggest that the phosphine is coordinated to the Ru atom (Scheme 2). Thus, the ^1H NMR resonance for the hydride ligand appears at δ −18.2, instead of ca. δ −20 to −22 in clusters of the type HRuCo₃(CO)₁₁L or HRuCo₃(CO)₁₀L₂ in which the ligand(s) L is bound to cobalt. Furthermore, the sharp $^{31}\text{P}\{^1\text{H}\}$ NMR resonance of **2b** contrasts with the quadrupole-broadened signals associated with cobalt-bound phosphorus nuclei.^{3a} Finally, the ^{59}Co NMR spectrum of **2b** consists of a broad resonance at δ −2790 ppm, whereas for **2a**, the expected two resonances are observed at δ −2719 ppm (Co–CO) and δ −2674 ppm (Co–P), in a 2:1 ratio.

These features distinguish **2b** from all the other known phosphine-monosubstituted RuCo₃ clusters, where Co is always the preferred coordination site, with the exception of RuCo₃(CO)₁₁(PMe₂Ph)($\mu_3\text{-AuPPh}_3$), in which the phosphine ligand PMe₂Ph was established by X-ray diffraction to be bound to Ru.⁸ In this case, however, steric effects might be at work. Thus, the bulky group AuPPh₃ may destabilize a phosphine bound to a Co atom and trigger its migration to Ru, whereas with the smaller hydride ligand, which is also μ_3 -bound to the cobalt face in the related HRuCo₃(CO)₁₁(PMe₂Ph), the expected isomer with the phosphine bound to Co was characterized by X-ray diffraction.⁹

The reactions of **1a** and **1b** with more than 2 equiv of PCyH₂ led to the formation of the disubstituted compounds HMC₃(CO)₁₀(PCyH₂)₂ (**3a**, M = Fe; **3b**, M = Ru). An interesting feature is that only the [Co, Co] isomer of **3a** was obtained, whereas **3b** was found *exclusively* as the [Co, Ru] isomer. This was established by comparison of their IR and multinuclear NMR data with those of HFeCo₃(CO)₁₀(PPh₂H)₂^{2a} and HRuCo₃(CO)₁₀(PMe₂Ph)₂^{2c} (see Table 1). Thus, the ^1H NMR resonance for the hydride ligand in **3b** appears at δ −18.6 ppm, instead of δ −21.9 ppm in **3a**. The sharp $^{31}\text{P}\{^1\text{H}\}$ NMR doublet for the Ru-bound P nucleus of **3b** is absent in **3a**, where only a broad resonance is observed at δ −40 ppm for the Co-bound P nuclei. These observations are consistent with previous results concerning the reaction of the Ru-bound telluride compound HRuCo₃(CO)₁₁(TeMe₂) with PMe₂Ph, which yielded only the disubstituted [Co, Ru] isomer.^{2c} For other clusters of the type HRuCo₃(CO)₁₀(Phosphine)₂, the structure of the preferred isomer depends on the nature of the phosphine. With, for example, PPh₃, the [Co, Co] isomer first formed was stable, whereas with, for example, PMe₂Ph or Ph₂PCH₂C(O)Ph, the [Co, Co] kinetic isomer slowly isomerized into the [Co, Ru] isomer.^{2c,5}

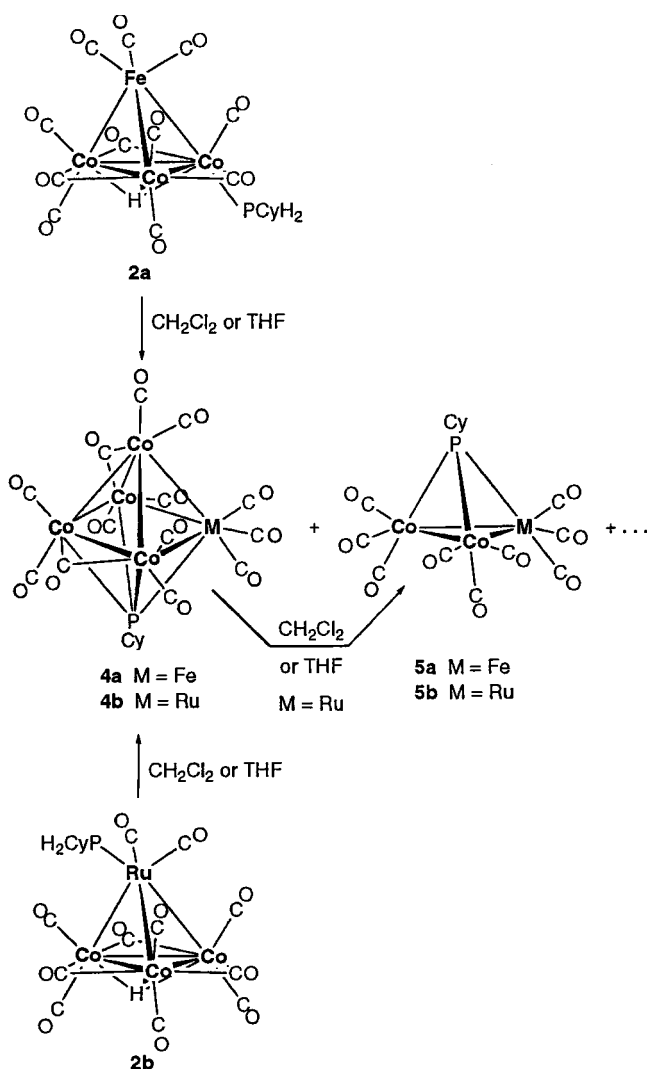
Isolated **2b** slowly transforms at room temperature in CH₂Cl₂ solution, more rapidly in THF, into two new species (a black and a yellow compound), as indicated by analytical thin-layer chromatography and monitoring by IR spectroscopy in the $\nu(\text{CO})$ region or by ^{59}Co NMR spectroscopy (Scheme 3). The black species was found

(7) Rossi, S.; Pursiainen, J.; Pakkanen, T. A. *J. Organomet. Chem.* **1990**, 397, 81.

(8) Kakkonen, H. J.; Ahlgren, M.; Pakkanen, T. A. *Acta Crystallogr.* **1994**, C50, 528.

(9) Pursiainen, J.; Ahlgren, M.; Pakkanen, T. A.; Valkonen, J. *J. Chem. Soc., Dalton Trans.* **1990**, 1147.

Scheme 3



to be a condensation product, the pentanuclear cluster RuCo₄(μ₄-PCy)(μ-CO)₂(CO)₁₁ (**4b**), which has been structurally characterized by X-ray diffraction (see below). Such a cluster expansion reaction has been previously observed in the reaction of Ru₃(CO)₁₂ with PPhH₂, which afforded tetranuclear and pentanuclear phosphinidene-capped homometallic clusters.^{6c} On the other hand, the yellow compound was found to be a heterometallic trinuclear cluster and characterized by X-ray diffraction as RuCo₂(μ₃-PCy)(CO)₉ (**5b**). This cluster results formally from the loss of two 12-valence-electron (12-VE) fragments Co(CO)₂⁺ from **4b**. The analogous clusters RuCo₂(μ₃-PR)(CO)₉ (R = Me, Ph) have been obtained by reaction of RuCo₂(CO)₁₁ with PRH₂ but were not characterized by X-ray diffraction.^{6e}

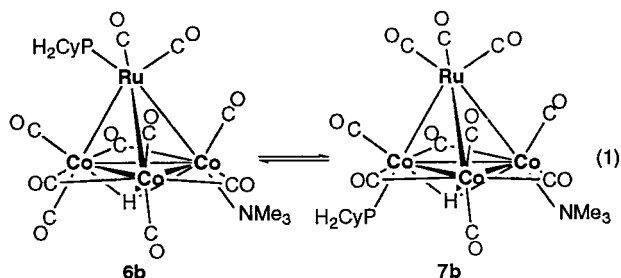
At the beginning of the transformation of **2b**, **5b** is only present in minor quantities compared to **4b**. This situation reverses with time, ending with complete conversion of **4b**. When pure **4b** was dissolved in CH₂Cl₂ or THF, it rapidly formed **5b**, which was the only species detected by ⁵⁹Co NMR spectroscopy, and some decomposition product that did not migrate on TLC plates (Scheme 3). This strongly suggests, but of course does not prove, that **5b** is formed via the intermediacy of **4b** and is not formed directly from **2b**. To see whether a bimolecular process, where a molecule of **1b** would

provide a fourth hydrogen and the Co(CO)₂ fragment necessary to complete the transformation of **2b** into **4b**, a 1:1 mixture of pure **1b** and **2b** was stirred in CH₂Cl₂ at room temperature for up to 7 days.²² We found that the presence of **1b** did not affect the course of the transformation of **2b**. When Co₂(CO)₈ was added to **2b** in CH₂Cl₂, the formation of the mixture **4b** + **5b** was slowed, until all Co₂(CO)₈ had been converted into Co₄(CO)₁₂. At this moment, the transformation of **2b** followed the normal course.

A similar behavior was observed with the iron-containing cluster **2a**, but in this case the formation of the intermediate condensation product FeCo₄(μ₄-PCy)(μ-CO)₂(CO)₁₁ (**4a**) was only detected using thin-layer chromatography and identified by comparison with **4b**. This unstable compound rapidly transforms into the phosphinidene-capped cluster FeCo₂(μ₃-PCy)(CO)₉ (**5a**), which was characterized by comparison with FeCo₂(μ₃-PPh)(CO)₉.¹⁰ The latter was prepared in a low yield (2.5%) by a completely different method, the reaction of PhP[Co(CO)₄]₂ with Fe₂(CO)₉.

Although the details of the mechanism leading to elimination of hydrogen are not known, it is reasonable to assume that the transformations leading to **4** and **5** involve initial P-H activation and CO substitution processes, giving MCo₃(μ-H)₂(μ-PCyH)(CO)₁₀ and finally MCo₃(μ-H)₃(μ₃-PCy)(CO)₉. Unfortunately, none of the expected intermediates has so far been observed. However, this hypothesis of stepwise P-H oxidative-addition reactions of a monosubstituted compound has been verified with the trinuclear clusters Os₃(CO)₁₁(PRH₂).^{6a}

The transformations of **2a** or **2b** may be easily accelerated by reaction with trimethylamine *N*-oxide. Thus, reaction of **2a** with a stoichiometric amount of Me₃NO led to CO₂ evolution and formation of a green solution characteristic for a disubstituted cluster. After a few minutes, the color of this solution rapidly turned deep red and the presence of cluster **5a** was indicated by TLC, together with a green spot attributed to HFeCo₃(CO)₁₀(NMe₃)(PCyH₂) by analogy with the known HFeCo₃(CO)₁₀(NMe₃)(PPh₂H).^{2a} However, ⁵⁹Co NMR monitoring of this reaction did not allow observation of the resonance of the amine-substituted cobalt atom. The reaction of **2b** with Me₃NO afforded the unstable phosphine-amine disubstituted cluster HRuCo₃(CO)₁₀(NMe₃)(PCyH₂) (**6b**), which was separated from decomposition products by extraction in nonpolar solvents such as toluene. Cluster **6b** was identified as the [Co, Ru] isomer, where the phosphine has remained on Ru and the amine ligand has substituted a Co-bound CO. This identification was done by comparison of its IR and ⁵⁹Co NMR data with those of the phosphine disubstituted cluster HRuCo₃(CO)₁₀(PMe₂Ph)₂, in which the [Co, Co] and [Co, Ru] isomers can be readily differentiated.^{2c} However, when the reaction of **2b** with Me₃NO was performed in an NMR tube for direct monitoring by ⁵⁹Co NMR, two new resonances were observed at δ -1150 ppm and -1360 ppm which are typical for amine-substituted Co atoms.^{2b} This may be explained by assuming that, in solution, this unstable cluster isomerizes, at least in part, to give a mixture of [Co, Co] and [Co, Ru] isomers (eq 1). For comparison, a similar sensitivity of the ⁵⁹Co NMR resonance of an amine-



substituted Co nucleus to the presence of a phosphine on an adjacent cobalt has been previously observed on going from the [Co, Co] isomer of $\text{HFeCo}_3(\text{CO})_{10}(\text{NMe}_3)(\text{PPh}_2\text{H})$ ($\delta -780$ ppm) to $\text{HFeCo}_3(\text{CO})_{11}(\text{NMe}_3)$ ($\delta -910$ ppm).^{2a}

The existence of **6b** supports our previous suggestion that the reaction of $\text{HRuCo}_3(\text{CO})_{11}(\text{PMe}_2\text{Ph})$ with Me_3NO occurs via a short-lived intermediate in which the phosphine has migrated to Ru.^{2c} The mixture of **6b** and **7b** transforms rapidly in solution ($t_{1/2} = 30$ min) into first **4b** and **5b** and eventually pure **5b**, as shown by ^{59}Co NMR spectroscopy, where the two additional resonances at $\delta -1805$ and -3030 ppm grew at the expense of those at $\delta -1150$ and -1360 ppm, reflecting the displacement of the Co-bound amine ligand.

Crystal Structures of $\text{RuCo}_4(\mu_4\text{-PCy})(\mu\text{-CO})_2(\text{CO})_{11}$ (4b**) and $\text{RuCo}_2(\mu_3\text{-PCy})(\text{CO})_9$ (**5b**).** The molecular structures of **4b** and **5b** have been determined by X-ray diffraction and are shown in Figures 1 and 2. Selected bond distances and angles are given in Tables 2 and 3, respectively.

In cluster **4b** the two crystallographically independent molecules in the asymmetric unit are structurally equivalent and are almost related to each other by a mirror plane, except for a slight rotation of the Cy substituent. The overall cluster geometry consists of a distorted octahedron with a cobalt atom and a phosphorus atom on opposite apexes, while the other four metal atoms form an approximately square-planar RuCo_3 array (Figure 1). Two Co–Co bonds are symmetrically bridged by a CO ligand, and the Co–Co distances range from $\text{Co}(1)\text{--Co}(3) = 2.493(2)$ Å to $\text{Co}(2)\text{--Co}(3) = 2.598(2)$ Å (molecule A). The other carbonyl ligands are terminally bound, two on each cobalt and three on ruthenium. The phosphinidene ligand caps the RuCo_3 plane in a slightly asymmetric manner such that one of the Co–P distances is shorter than the other two (see Table 2). The Ru–P(1) distance of $2.305(3)$ Å ($2.273(3)$ Å in molecule B) is shorter than in the cluster $\text{Ru}_5(\mu_4\text{-PPh})(\text{CO})_{15}$ ($2.339(6)\text{--}2.407(7)$ Å).¹¹ The P(1)–C(14) distance of $1.85(1)$ Å ($1.89(1)$ Å in molecule B) involving the phosphinidene ligand is comparable to that previously reported in the only other structurally characterized cluster with a $\mu_4\text{-PCy}$ ligand, $\text{Ru}_4(\mu_4\text{-PCy})_2(\mu\text{-PCy})_2(\text{CO})_8$.¹² Cluster **4b** has 7 electron pairs, consistent with a *nido* octahedron for the five metal atoms or a *closo* octahedron when the P atom is considered as part of the skeleton. The metal atoms all obey the 18-electron rule.

Cluster **5b** contains a triangular core with one ruthenium and two cobalt atoms. The position of the

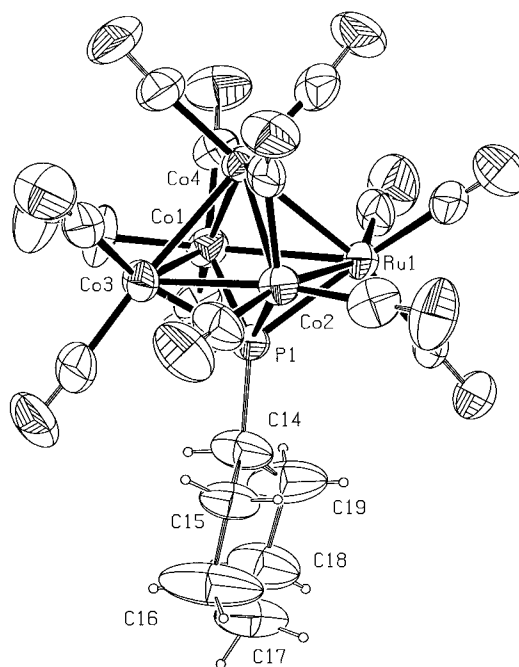


Figure 1. ORTEP view of one molecule of $\text{RuCo}_4(\mu_4\text{-PCy})(\mu\text{-CO})_2(\text{CO})_{11}$ (**4b**) with the atom-labeling scheme (50% probability ellipsoids).

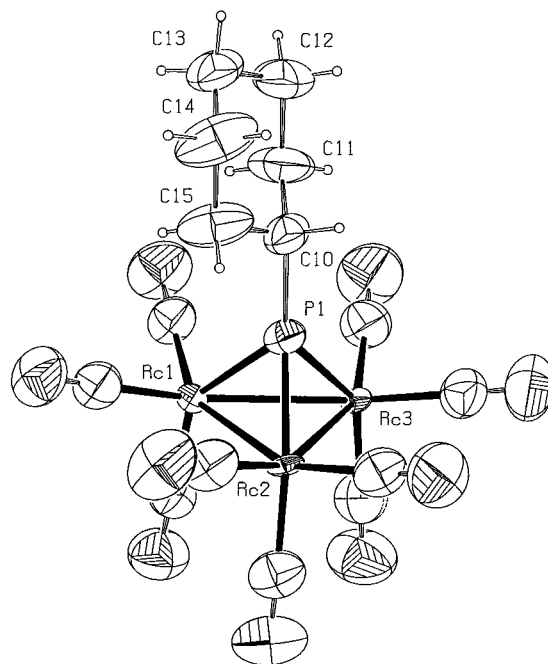


Figure 2. ORTEP view of one molecule of $\text{RuCo}_2(\mu_3\text{-PCy})(\text{CO})_9$ (**5b**) with the atom-labeling scheme (50% probability ellipsoids).

ruthenium atom is statistically disordered over all three metal sites with a pseudo atom named RC ($\text{RC} = \frac{1}{3}\text{Ru} + \frac{2}{3}\text{Co}$) representing this metal site (Figure 2). Related disorder problems have been encountered with $\text{H}_2\text{-RuOs}_3(\text{CO})_{13}$ and $(\text{AsPh}_4)[\text{H}_3\text{RuOs}_3(\text{CO})_{12}]$.¹³ The average metal–metal bond distance of 2.648 Å is intermediate between a Co–Co and a Ru–Co bond length in **4b**. Each metal atom bears three terminal carbonyl groups. As in $\text{FeCo}_2(\mu_3\text{-PPh})(\text{CO})_9$,¹⁴ the phosphorus

(11) Natarajan, K.; Zsolnai, L.; Huttner, G. *J. Organomet. Chem.* **1981**, 209, 85.

(12) Beguin, A.; Rheinwald, G.; Stoeckli-Evans, H.; Süss-Fink, G. *Helv. Chim. Acta* **1994**, 77, 525.

(13) Rheingold, A. L.; Gates, B. C.; Scott, J. P.; Budge, J. R. *J. Organomet. Chem.* **1987**, 331, 81.

Table 2. Selected Bond Distances (Å) and Angles (deg) for RuCo₄(μ₄-PCy)(μ-CO)₂(CO)₁₁ (4b**)**

	molecule			molecule	
	A	B		A	B
Bond Distances					
Ru(1)–Co(1)	2.771(2)	2.684(2)	Co(2)–Co(4)	2.533(2)	2.535(2)
Ru(1)–Co(2)	2.707(2)	2.677(2)	Co(2)–P(1)	2.241(3)	2.256(3)
Ru(1)–Co(4)	2.699(2)	2.666(2)	Co(2)–C(7)	1.76(1)	1.76(1)
Ru(1)–P(1)	2.305(3)	2.273(3)	Co(2)–C(8)	1.76(2)	1.74(2)
Ru(1)–C(1)	1.91(1)	1.88(2)	Co(2)–C(9)	1.92(1)	1.90(1)
Ru(1)–C(2)	1.89(1)	1.93(2)	Co(3)–Co(4)	2.557(2)	2.605(2)
Ru(1)–C(3)	1.97(1)	1.88(2)	Co(3)–P(1)	2.204(3)	2.238(3)
Co(1)–Co(3)	2.493(2)	2.553(2)	Co(3)–C(6)	1.87(1)	1.87(1)
Co(1)–Co(4)	2.498(2)	2.499(2)	Co(3)–C(10)	1.79(1)	1.80(1)
Co(1)–P(1)	2.252(3)	2.236(3)	Co(3)–C(11)	1.80(2)	1.82(1)
Co(1)–C(4)	1.76(1)	1.80(1)	Co(4)–C(9)	1.99(1)	1.98(1)
Co(1)–C(5)	1.76(1)	1.72(1)	Co(4)–C(12)	1.80(1)	1.80(1)
Co(1)–C(6)	1.88(1)	2.24(2)	Co(4)–C(13)	1.83(1)	1.77(2)
Co(2)–Co(3)	2.598(2)	2.638	P(1)–C(14)	1.85(1)	1.89(1)
Bond Angles					
Co(1)–Ru(1)–Co(2)	83.89(5)	85.88(6)	Co(4)–Co(2)–P(1)	78.4(1)	78.49(9)
Co(1)–Ru(1)–P(1)	51.69(8)	52.84(8)	P(1)–Co(2)–C(7)	110.0(5)	111.5(4)
Co(2)–Ru(1)–P(1)	52.37(8)	53.48(8)	P(1)–Co(2)–C(8)	119.4(4)	114.8(5)
Co(4)–Ru(1)–P(1)	73.91(8)	75.47(9)	P(1)–Co(2)–C(9)	128.9(4)	128.8(4)
P(1)–Ru(1)–C(1)	119.0(4)	110.7(6)	Co(1)–Co(3)–Co(2)	91.89(9)	89.42(7)
P(1)–Ru(1)–C(2)	94.7(3)	90.8(4)	Co(1)–Co(3)–Co(4)	59.27(8)	57.95(6)
P(1)–Ru(1)–C(3)	144.0(4)	150.3(4)	Co(1)–Co(3)–P(1)	56.9(1)	55.17(9)
Ru(1)–Co(1)–Co(3)	92.35(6)	93.8(7)	Co(1)–Co(3)–C(6)	48.5(4)	58.4(5)
Ru(1)–Co(1)–Co(4)	61.36(5)	61.80(6)	Co(2)–Co(3)–Co(1)	91.95(7)	89.42(7)
Ru(1)–Co(1)–P(1)	53.43(8)	54.10(9)	Co(2)–Co(3)–Co(4)	58.84(6)	57.83(5)
Co(3)–Co(1)–Co(4)	61.65(6)	62.07(6)	Co(2)–Co(3)–P(1)	54.89(9)	54.37(9)
Co(3)–Co(1)–P(1)	55.07(8)	55.25(9)	Co(4)–Co(3)–P(1)	78.50(9)	77.33(9)
Co(3)–Co(1)–C(6)	48.1(4)	45.4(4)	P(1)–Co(3)–C(6)	101.7(4)	107.7(5)
Co(4)–Co(1)–P(1)	78.91(9)	79.65(9)	P(1)–Co(3)–C(10)	154.6(5)	148.1(4)
P(1)–Co(1)–C(4)	101.6(4)	106.8(4)	P(1)–Co(3)–C(11)	97.0(4)	96.1(5)
P(1)–Co(1)–C(5)	150.1(4)	150.8(4)	Ru(1)–Co(4)–Co(1)	64.30(5)	62.52(7)
P(1)–Co(1)–C(6)	99.6(5)	96.1(4)	Ru(1)–Co(4)–Co(2)	62.22(5)	61.89(6)
Ru(1)–Co(2)–Co(3)	91.55(6)	91.33(6)	Ru(1)–Co(4)–Co(3)	92.63(6)	92.32(6)
Ru(1)–Co(2)–Co(4)	61.90(5)	61.46(6)	Co(1)–Co(4)–Co(2)	93.40(7)	93.03(7)
Ru(1)–Co(2)–P(1)	54.56(8)	54.05(8)	Co(1)–Co(4)–Co(3)	59.07(6)	59.98(7)
Co(3)–Co(2)–Co(4)	59.77(6)	60.42(5)	Co(2)–Co(4)–Co(3)	61.39(6)	61.75(5)
Co(3)–Co(2)–P(1)	53.57(8)	53.74(9)	Co(1)–Co(4)–C(9)	140.9(4)	140.1(4)

Table 3. Selected Bond Distances (Å) and Angles (deg) for RuCo₂(μ₃-PCy)(CO)₉ (5b**)**

Bond Distances			
RC(1)–RC(2)	2.641(2)	RC(1)–C(3)	1.818(5)
RC(1)–RC(3)	2.647(1)	RC(2)–C(7)	1.842(5)
RC(2)–RC(3)	2.655(1)	RC(2)–C(8)	1.839(5)
RC(1)–P(1)	2.180(2)	RC(2)–C(9)	1.825(5)
RC(2)–P(1)	2.173(1)	RC(3)–C(4)	1.820(5)
RC(3)–P(1)	2.176(1)	RC(3)–C(5)	1.849(6)
RC(1)–C(1)	1.812(5)	RC(3)–C(6)	1.834(5)
RC(1)–C(2)	1.823(5)	P(1)–C(10)	1.836(4)
Bond Angles			
RC(2)–RC(1)–RC(3)	60.26(4)	RC(3)–RC(2)–P(1)	52.43(4)
RC(2)–RC(1)–P(1)	52.53(4)	RC(3)–RC(2)–C(7)	98.0(2)
RC(2)–RC(1)–C(1)	151.8(2)	RC(3)–RC(2)–C(8)	97.7(2)
RC(2)–RC(1)–C(2)	97.4(2)	RC(3)–RC(2)–C(9)	153.1(2)
RC(2)–RC(1)–C(3)	96.4(2)	RC(1)–RC(3)–RC(2)	59.77(3)
RC(3)–RC(1)–P(1)	52.51(4)	RC(1)–RC(3)–P(1)	52.64(5)
RC(3)–RC(1)–C(1)	96.8(2)	RC(1)–RC(3)–C(4)	98.7(2)
RC(3)–RC(1)–C(2)	152.1(2)	RC(1)–RC(3)–C(5)	96.5(2)
RC(3)–RC(1)–C(3)	96.4(2)	RC(1)–RC(3)–C(6)	153.7(2)
RC(1)–RC(2)–RC(3)	59.98(4)	RC(2)–RC(3)–P(1)	52.34(4)
RC(1)–RC(2)–P(1)	52.76(4)	RC(2)–RC(3)–C(4)	153.4(2)
RC(1)–RC(2)–C(7)	96.4(2)	RC(2)–RC(3)–C(5)	97.4(2)
RC(1)–RC(2)–C(8)	153.7(2)	RC(2)–RC(3)–C(6)	98.4(2)
RC(1)–RC(2)–C(9)	98.8(2)		

atom of the μ₃-phosphinidene ligand caps symmetrically the trimetal plane with an average RC–P(1) bond distance of 2.176 Å which is significantly shorter than the Co–P or Ru–P bond distances in cluster **4b**. As expected, the μ₃-P(1)–C(10) distance of 1.836(4) Å is slightly shorter than the μ₄-P–C(14) distance in **4b** and

is comparable to those observed in other μ₃-PR ligands.^{6b,14} Cluster **5b** has 6 electron pairs, consistent with an *arachno* trigonal bipyramid for the three metal atoms or a *nido* trigonal bipyramid when the P atom is considered as part of the skeleton. As in **4b**, the metal atoms all obey the 18-electron rule.

Conclusion

We have observed that monosubstitution of HMC₃–(CO)₁₂ with PCyH₂ occurs with a different metallosite selectivity as a function of M = Fe, Ru. In the former case, substitution of a Co-bound CO ligand occurs, whereas when M = Ru, the phosphine ligand is bound to Ru. This reaction appears to be under thermodynamic control. Introduction of a second substituent (PCyH₂ or NMe₃) occurs in both cases at cobalt and, in the case of HFeCo₃(CO)₁₁(PCyH₂), at a cobalt that does not carry the PCyH₂ substituent. The clusters HMC₃(CO)₁₁–(PCyH₂) (**2a**, M = Fe; **2b**, M = Ru) transform in solution to give the corresponding μ₃-phosphinidene-capped heterotrimeric clusters MCo₂(μ₃-PCy)(CO)₉ (**5a**, M = Fe; **5b**, M = Ru). When M = Ru, a pentanuclear intermediate could be isolated and characterized by X-ray diffraction as the μ₄-phosphinidene-capped cluster RuCo₄–(μ₄-PCy)(μ-CO)₂(CO)₁₁ (**4b**). The analogous species could

(14) Beurich, H.; Madach, T.; Richter, F.; Vahrenkamp, H. *Angew. Chem., Int. Ed. Engl.* **1979**, *18*, 690.

not be isolated when $M = \text{Fe}$, owing to its lability. The transformation of **2a,b** was accelerated by addition of Me_3NO , which generated a labile phosphine–amine intermediate. We believe that a significant aspect of this work is the demonstration that a reaction which represents a cluster partial fragmentation, with nuclearity change from 4 to 3, may occur via the intermediacy of a larger cluster, of nuclearity 5. This observation may bear relevance to a number of rearrangement processes in cluster chemistry and be more general than previously thought.

Experimental Section

General Procedures. Reactions and manipulations, except chromatographic separations, were carried out under N_2 using standard Schlenk tube techniques. Solvents were distilled before use. $\text{HFeCo}_3(\text{CO})_{12}^{15}$ and $\text{HRuCo}_3(\text{CO})_{12}^{2a}$ were prepared according to published procedures. PCyH_2 was commercially available and used as received. Solution infrared spectra were recorded on a Nicolet 20SXC or a Bruker IFS-66 FT IR spectrometer. ^1H and $^{31}\text{P}\{^1\text{H}\}$ NMR spectra were recorded at 300.17 and 121.5 MHz, respectively, on a Bruker AC-300 spectrometer using CDCl_3 as the solvent. Chemical shifts are relative to TMS and H_3PO_4 , respectively. ^{59}Co NMR spectra were measured on a Bruker MSL-300 instrument (71.21 MHz). The chemical shifts reported (ppm) for ^{59}Co are positive high frequency from the external reference $\text{K}_3[\text{Co}(\text{CN})_6]$ saturated in D_2O . Standard parameters are as follows: pulse width 3 μs , sweep width 263 kHz, number of scans between 5000 and 100 000. Selected physical and spectroscopic data for the complexes are given in Table 1. When the product stability allowed, elemental analyses are given. The progress of the reactions was monitored by analytical thin-layer chromatography (5554 Kieselgel 60F₂₅₄, Merck), and the products were separated on 20×20 cm glass plates coated with Kieselgel 60F₂₅₄.

Preparation of $\text{HFeCo}_3(\text{CO})_{11}(\text{PCyH}_2)$ (2a**).** $\text{HFeCo}_3(\text{CO})_{12}$ (**1a**; 0.331 g, 0.581 mmol) was dissolved in CH_2Cl_2 (40 mL), and PCyH_2 (0.077 mL, 0.581 mmol) was added. After the mixture was stirred for 0.5 h at room temperature, the dark violet solution was filtered and the solvent was evaporated in vacuo. The resulting solid was extracted with hexane (40 mL), and this solution was placed at -15°C overnight, giving black crystals of **2a** (0.155 g, 45%). Anal. Calcd for $\text{C}_{17}\text{H}_{14}\text{Co}_3\text{FeO}_{11}\text{P}$: C, 31.04; H, 2.15. Found: C, 30.8; H, 2.2.

Preparation of $\text{HRuCo}_3(\text{CO})_{11}(\text{PCyH}_2)$ (2b**).** $\text{HRuCo}_3(\text{CO})_{12}$ (**1b**; 0.240 g, 0.390 mmol) was dissolved in CH_2Cl_2 (20 mL), and PCyH_2 (0.052 mL, 0.391 mmol) was added. The wine red solution, which became immediately dark red, was stirred for 0.5 h at room temperature. The solution was filtered, and the solvent was evaporated in vacuo. The resulting solid was extracted with hexane (20 mL), and this solution was placed at -15°C overnight, giving black crystals of **2b** (0.170 g, 62%). Anal. Calcd for $\text{C}_{17}\text{H}_{14}\text{Co}_3\text{O}_{11}\text{PRu}$: C, 29.04; H, 2.01. Found: C, 29.5; H, 2.1.

Preparation of $\text{HFeCo}_3(\text{CO})_{10}(\text{PCyH}_2)_2$ (3a**).** $\text{HFeCo}_3(\text{CO})_{12}$ (**1a**; 0.231 g, 0.405 mmol) was dissolved in CH_2Cl_2 (30 mL), and PCyH_2 (0.137 mL, 1.04 mmol) was added. After the mixture was stirred for 1 h at room temperature, the TLC plates indicated the formation of one major dark violet compound. The solution was filtered, and the solvent was evaporated in vacuo. The resulting oil was extracted with hexane (60 mL), and this solution was placed at -15°C overnight, giving a black powder of **3a** (0.162 g, 54%). Anal. Calcd for $\text{C}_{22}\text{H}_{27}\text{Co}_3\text{FeO}_{10}\text{P}_2$: C, 35.42; H, 3.65. Found: C, 35.7, H, 3.8.

Preparation of $\text{HRuCo}_3(\text{CO})_{10}(\text{PCyH}_2)_2$ (3b**).** $\text{HRuCo}_3(\text{CO})_{12}$ (**1b**; 0.100 g, 0.163 mmol) was dissolved in CH_2Cl_2 (20

mL), PCyH_2 (0.043 mL, 0.326 mmol) was added, and the solution was stirred at room temperature. The reaction was monitored by TLC plates, which indicated the formation of two major products: the monosubstituted **2b** followed by the disubstituted compound **3b**. After being stirred for 2 h, the dark red solution was filtered and the solvent evaporated in vacuo. Chromatographic separation, with hexane/ CH_2Cl_2 (80/20) as eluant, yielded pure **3b** (0.035 g, 27%). However, this compound was highly unstable in the solid state as well as in solution.

Prolonged reaction times or the use of an excess of PCyH_2 did not improve the yield and favored the formation of a new compound (probably a trisubstituted derivative not further investigated) together with some decomposition.

Preparation of $\text{RuCo}_4(\mu_4\text{-PCy})(\mu\text{-CO})_2(\text{CO})_{11}$ (4b**).** $\text{HRuCo}_3(\text{CO})_{12}$ (**1b**; 0.320 g, 0.520 mmol) was dissolved in CH_2Cl_2 (30 mL), and PCyH_2 (0.069 mL, 0.520 mmol) was added. After the solution was stirred for 0.5 h at room temperature, the solution was filtered and the solvent was evaporated in vacuo. The resulting solid was extracted with toluene (30 mL), and this solution was placed at -15°C . After 1 week the toluene was evaporated; the solid residue was dissolved in CH_2Cl_2 (20 mL) and this solution stored 1 week at room temperature. The presence of two new products together with the monosubstituted compound **2b** was indicated by TLC. The solvent was evaporated, and the solid residue was extracted with hexane. The resulting solution was placed at -15°C overnight, giving black needles of **4b** (0.080 g, 19%). Anal. Calcd for $\text{C}_{19}\text{H}_{11}\text{Co}_4\text{O}_{13}\text{-PRu}$: C, 28.00; H, 1.36. Found: C, 28.5, H, 1.4. FAB-MS: m/z 815 (10%, M^+), 787 (74%, $\text{M}^+ - \text{CO}$), 759 (100%, $\text{M}^+ - 2\text{CO}$), 731 (96%, $\text{M}^+ - 3\text{CO}$), 703 (52%, $\text{M}^+ - 4\text{CO}$), 675 (45%, $\text{M}^+ - 5\text{CO}$).

Preparation of $\text{FeCo}_2(\mu_3\text{-PCy})(\text{CO})_9$ (5a**).** $\text{HFeCo}_3(\text{CO})_{11}(\text{PCyH}_2)$ (**2a**; 0.050 g, 0.076 mmol) was dissolved in THF (10 mL), and the solution was stirred at room temperature for 2 days. The progressive formation of a new brown-violet compound was monitored by TLC. The solution was filtered, and the solvent was evaporated in vacuo. The resulting solid was extracted with hexane (10 mL), and this solution was placed at -15°C for 2 days, giving black crystals of **5a** (0.024 g, 58%). Anal. Calcd for $\text{C}_{15}\text{H}_{11}\text{Co}_2\text{FeO}_9\text{P}$: C, 33.34; H, 2.05. Found: C, 33.7; H, 2.5.

Preparation of $\text{RuCo}_2(\mu_3\text{-PCy})(\text{CO})_9$ (5b**).** $\text{HRuCo}_3(\text{CO})_{11}(\text{PCyH}_2)$ (**2b**; 0.050 g, 0.071 mmol) was dissolved in THF (20 mL). The solution was stirred at room temperature. The progressive formation of a new orange compound was monitored by TLC. After 2 days, the resulting solution was evaporated to dryness and the solid residue was extracted with hexane. This solution, placed overnight at -15°C , afforded orange crystals of **5b** (0.017 g, 42%). Anal. Calcd for $\text{C}_{15}\text{H}_{11}\text{-Co}_2\text{O}_9\text{PRu}$: C, 30.79; H, 1.90. Found: C, 31.0; H, 2.2. FAB-MS: m/z 585 (40%, M^+), 557 (100%, $\text{M}^+ - \text{CO}$), 529 (80%, $\text{M}^+ - 2\text{CO}$), 501 (20%, $\text{M}^+ - 3\text{CO}$).

Reaction of $\text{HRuCo}_3(\text{CO})_{11}(\text{PCyH}_2)$ with Me_3NO . Solid Me_3NO was added to a solution of $\text{HRuCo}_3(\text{CO})_{11}(\text{PCyH}_2)$ (**1b**; 0.040 g, 0.057 mmol) in CH_2Cl_2 (10 mL). Evolution of CO_2 occurred immediately, and the wine red solution became violet. After the solution was stirred for 0.25 h at room temperature, it was evaporated in vacuo. The resulting solid was extracted with hexane (20 mL), and this solution was placed at -15°C for 12 h, giving black crystals of $\text{HRuCo}_3(\text{CO})_{11}(\text{NMe}_3)(\text{PCyH}_2)$ (**6b**; 0.020 g, 50%). Anal. Calcd for $\text{C}_{19}\text{H}_{23}\text{NCo}_3\text{O}_{10}\text{PRu}$: C, 31.08; H, 3.16; N, 1.91. Found: C, 31.6; H, 3.4; N, 2.1.

X-ray Crystallography. Suitable black crystals of **4b** and **5b** were obtained by slow crystallization from a CH_2Cl_2 /hexane solution at -15°C . Diffraction measurements were carried out at room temperature on an automatic Nonius CAD-4 diffractometer using graphite-monochromated $\text{Mo K}\alpha$ radiation.¹⁶

(15) Chini, P.; Colli, L.; Peraldo, M. *Gazz. Chim. Ital.* **1960**, *90*, 1005.

(16) Fair, C. K. *MoLEN: An Interactive Intelligent System for Crystal Structure Analysis*; Enraf-Nonius, Delft, The Netherlands, 1990.

Table 4. Crystallographic Data for RuCo₄(μ₄-PCy)(μ-CO)₂(CO)₁₁ (4b) and RuCo₂(μ₃-PCy)(CO)₉ (5b)

	4b	5b
formula	RuCo ₄ C ₁₉ H ₁₁ O ₁₃ P	RuCo ₂ C ₁₅ H ₁₁ O ₉ P
fw	815.06	585.2
temp (K)	293(2)	293(2)
wavelength (Å)	0.71069	0.71069
cryst syst	triclinic	triclinic
space group	<i>P</i> 1	<i>P</i> 1
<i>a</i> (Å)	9.103(3)	8.119(2)
<i>b</i> (Å)	16.425(2)	8.124(6)
<i>c</i> (Å)	17.708(2)	17.709(6)
α (deg)	91.12(1)	86.34(3)
β (deg)	91.13(2)	83.61(3)
γ (deg)	99.66(2)	63.52(4)
<i>V</i> (Å ³)	2609(1)	1039(1)
<i>Z</i>	4	2
calcd density (Mg/m ³)	2.075	1.871
abs coeff (mm ⁻¹)	3.180	2.411
<i>F</i> (000)	1584	572
cryst size (mm)	0.35 × 0.25 × 0.09	0.25 × 0.22 × 0.10
θ range for data collecn (deg)	1.15–22.97	1.16–26.97
limiting indices	0 ≤ <i>h</i> ≤ 9, −18 ≤ <i>k</i> ≤ 17, −19 ≤ <i>l</i> ≤ 19	0 ≤ <i>h</i> ≤ 10, −9 ≤ <i>k</i> ≤ 10, −22 ≤ <i>l</i> ≤ 22
no. of rflns	7761/7218	4861/4530
colld/unique	(<i>R</i> (int) = 0.0183)	(<i>R</i> (int) = 0.0148)
completeness to θ _{max}	100.0	100.0
refinement method	full-matrix least squares on <i>F</i> ²	
no. of data/restraints/params	7218/0/686	4530/0/255
goodness of fit on <i>F</i> ²	1.075	1.069
final <i>R</i> indices	<i>R</i> 1 = 0.0551, <i>wR</i> 2 = 0.1649	<i>R</i> 1 = 0.0389, <i>wR</i> 2 = 0.1162
<i>R</i> indices (all data)	<i>R</i> 1 = 0.1167, <i>wR</i> 2 = 0.1894	<i>R</i> 1 = 0.0529, <i>wR</i> 2 = 0.1237
extinction coeff	0.0000(2)	0.0067(13)
largest diff peak and hole, e Å ⁻³	1.881 and −1.509	0.977 and −0.580

The cell parameters are obtained by fitting a set of 25 high-θ reflections. The intensities of three reflections were monitored every 1 h of exposure and showed no evidence of decay. Crystal data and intensity collection parameters are given in Table 4. Atomic scattering factors were taken from ref 17. Ortep plots were obtained using PLATON98.¹⁸ All the calculations were performed on a Silicon Graphics Indy computer.

Structure Analysis and Refinement. Compound 4b.

Data collection parameters are given in Table 4. 2θ_{max} = 54°, scan ω/2θ = 1, and *t*_{max} = 60 s; intensity controls without appreciable decay (1.5%) give 7761 reflections, from which 7218 were independent (4565 with *I* > 2σ(*I*)). After Lorentz and polarization corrections and absorption corrections with

ψ scan,¹⁹ the structure was solved with SIR-97, which revealed the non-hydrogen atoms of the structure.²⁰ After anisotropic refinement, all the hydrogen atoms were found by a difference Fourier synthesis. The whole structure was refined with SHELXL97,²¹ by full-matrix least-squares techniques (use of *F* magnitude; *x*, *y*, *z*, β_{*ij*} for Ru, Co, P, O, and C atoms and *x*, *y*, *z* in riding mode for H atoms): 686 variables and 4565 observations; *w*(calcd) = 1/[σ²(*F*_o²) + (0.1271*P*)²], where *P* = (*F*_o² + 2*F*_c²)/3 with the resulting *R* = 0.055, *R*_w = 0.164, and GOF = 1.075 (residual Δρ ≤ 1.88 e Å⁻³).

Compound 5b. Data collection parameters are given in Table 4. 2θ_{max} = 54°, scan ω/2θ = 1, and *t*_{max} = 60 s; intensity controls without appreciable decay (1.0%) give 4861 reflections, of which 4530 were independent (3743 with *I* > 2σ(*I*)). After Lorentz and polarization corrections and absorption corrections with ψ scan,¹⁹ the structure was solved with SIR-97, which revealed the non-hydrogen atoms of the structure.²⁰ During the calculations, the Ru and Co atoms appeared statistically disordered; therefore, a pseudo atom named RC was created (RC = ¹/₃ Ru + ²/₃ Co). After anisotropic refinement, all the hydrogen atoms are found by a difference Fourier synthesis. The whole structure was refined with SHELXL97,²¹ by full-matrix least-squares methods (use of *F* magnitude; *x*, *y*, *z*, β_{*ij*} for Ru, Co, P, O, and C atoms and *x*, *y*, *z* in riding mode for H atoms): 255 variables and 3743 observations; *w*(calcd) = 1/[σ²(*F*_o²) + (0.0787*P*)² + 0.8325*P*], where *P* = (*F*_o² + 2*F*_c²)/3 with the resulting *R* = 0.039, *R*_w = 0.116, and GOF = 1.069 (residual Δρ ≤ 0.97 e Å⁻³).

Acknowledgment. We are grateful to Prof. P. Granger and Drs. J. Raya and T. Richert (Strasbourg, France) for their contribution to the ⁵⁹Co NMR study and to the CNRS, the Ministère de l'Éducation Nationale, de l'Enseignement Supérieur et de la Recherche, the Ministère des Affaires Étrangères (Paris), and the Ministère des Affaires Étrangères (Alger) for support of the Strasbourg-Constantine Cooperation Project 96 MDU 371.

Supporting Information Available: Tables giving details of the structure determination, atomic coordinates, including those of the hydrogen atoms, anisotropic thermal parameters, and all bond distances and angles for complexes **4b** and **5b**. This material is available free of charge via the Internet at <http://pubs.acs.org>.

OM9902840

(19) Spek, A. L. HELENA: Program for the Handling of CAD4-Diffractometer Output SHELX(S/L); Utrecht University, Utrecht, The Netherlands, 1997.

(20) Altomare, A.; Burla, M. C.; Camalli, M.; Casciarano, G.; Giacivazzo, C.; Guagliardi, A.; Moliterni, A. G. G.; Polidori, G.; Spagna, R. SIR97: a New Tool for Crystal Structure Determination and Refinement. *J. Appl. Crystallogr.* **1998**, *31*, 7477.

(21) Sheldrick, G. M. SHELXL93: Program for the Refinement of Crystal Structures; University of Göttingen, Göttingen, Germany, 1993.

(22) We are grateful to a reviewer for suggesting this experiment.

(17) *International Tables for X-ray Crystallography*; Kynoch Press: Birmingham, U.K., 1974; Vol. IV, p 99.

(18) Spek, A. L. PLATON: A Multipurpose Crystallographic Tool; Utrecht University, Utrecht, The Netherlands, 1998.